Challenging Glass 7
Conference on Architectural and Structural Applications of Glass
Belis, Bos & Louter (Eds.), Ghent University, September 2020.

ISBN 978-94-6366-296-3, https://doi.org/10.7480/cgc.7.4713

Dynamic Behavior of Laminated Glass Plates

Claude Boutin, Kevin Viverge
Université de Lyon – ENTPE, LGCB/LTDS UMRCNRS 5513, France. claude.boutin@entpe.fr

This paper dealt with the theoretical and experimental dynamic behaviour of laminated glass. The developments are based on the contrasted plate model (Boutin and Viverge 2016) that accounts for the high contrast of mechanical properties between the glass layers and the soft viscoelastic interlayer through the additional kinematic variable describing the sliding between the glass layers. This yields an analytic tri-Laplacian representation that encompasses (i) the shear related to the sliding within the PVB, (ii) the local bending of each glass layer, and (iii) global bending of the whole laminate. In dynamics it is shown that three types of bending waves exist, two being evanescent and one being propagating. This enables the determination of the modes of laminated glass plates submitted to different boundary conditions. The energy balance enables to assess the local dissipation of the PVB, which results in the damping of the modes. This approach is compared to vibration tests performed at temperatures ranging from 30 to 50°C. The influence of the PVB on the eigen frequencies and on the damping is clearly evidenced. A good qualitative correspondence with the theory is obtained.

Keywords: Laminated glass, Dynamics, Visco-elasticity, Tri-Laplacian plate

1. Introduction

Laminated glass plates belong to a specific category of stratified media, the constituents of which present highly contrasted mechanical properties. Due to the weak stiffness of the thin polymeric central layer compared to the strong stiffness of the glass layer, the usual assumptions at the basis of the classical plate models have to be reconsidered (Berdichevsky 2010). To address this question, numerical, phenomenological, and theoretical has been developed, see e. g. (Carrera 2003; Carrera and Ciuffreda 2005; Foraboschi 2012; Galuppi and Royer-Carfagni 2012; Ivanov 2006). Among the theoretical ones, we consider here the recent works (Boutin and Viverge 2016) performed in the framework of a two-scale asymptotic analysis enabling the dimension reduction from 3D description of the materials to the 2D description of the laminated plate. This approach enables to handle in a same way the two main difficulties of the laminated glass plates, namely the specific kinematics and the viscoelastic properties.

In the present paper we extend these previous developments to investigates theoretically the dynamic behavior of such laminates. Experiments are also conducted in view of validating the theoretical outcomes.

The paper is organized as follows. Section 2 recall the aspects of the contrasted plate model. Section 3, deals with the bending waves in such plates in general case, while Sections 4 and 5 focus on the features of the bending waves and eigen modes in the specific cases of elastic contrasted plates and of laminated glass. Section 6 presents the performed dynamic tests and a comparison of the experimental data and the theoretical assessment.

2. Summary of the contrasted plate model

The 2D effective plate behavior is derived from the 3D constitutive law of the materials through an asymptotic method of dimension (Ciarlet and Destuynder 1979; Ciarlet 1997). This theoretical method is inspired from the homogenization method (Sanchez-Palencia 1980; Caillerie 1982; Auriault et al. 2009) and developed in the framework of small deformations. The contrast of mechanical properties is accounted for by an appropriate scaling of the stiffness (Berdichevsky 2010; Boutin and Viverge 2016). The relevancy of this model for laminated glass has been checked experimentally owing to static bending tests and to creep bending tests (Viverge et al. 2016). The main outcomes of this theoretical approach are summarized here-below, considering for simplicity symmetric plates made of two stiff layers each of thickness h, and a thin central layer of thickness c. For clarity the case of an elastic soft central layer is first addressed.

2.1. Elastic contrasted plate

Due to the large softness of the central layer, in addition to the two kinematic descriptors of classical plate model, namely the out of plane deflection $w(x,y)$, and the deflection's gradient $\nabla w(x,y)$, a third kinematic descriptor $\boldsymbol{d}(x,y)$ is required, that describes the sliding vector, i.e. the differential in-plane motion, between the two glass layers. Hence, the overall rotation vector of the normal fiber reads $\boldsymbol{\alpha} = \nabla w - \boldsymbol{d}/(h+c)$. In parallel, the forces and momentum duals to these kinematic descriptors are:

- the overall momentum tensor **M**, dual to the overall rotation vector $\boldsymbol{\alpha}$,
- the inner momentum tensor **M**, dual to the gradient of deflection ∇w,
- the inner shear force **T**, dual to the sliding vector $\boldsymbol{d}$,

the constitutive laws of which are explicitly determined from the mechanical properties and the geometry of the layers. They read as follows in the case of elastic constituents, including the soft central layer:

$$\mathbf{M} = E_0(\Im - 2I)\,\mathbf{E}(\boldsymbol{\alpha}) \;;\quad \mathbf{M} = 2E_0 I\,\mathbf{E}(\nabla w) \;;\quad \mathbf{T} = \mu(h+c)d/c = K(\nabla w - \boldsymbol{\alpha}) \;;\quad K = \mu(h+c)^2/c \qquad (1)$$

In these expressions:

- E, ν, and $E_0 = E(1-\nu^2)$ stand respectively for the Young modulus, the Poisson ratio and the apparent plate modulus of the glass,
- $I = h^3/12$ and $\Im = 2I + h(h+c)^2/2$ are respectively the inertia of a single glass layer, and the inertia of the whole laminate,
- for any in-plane vector $\boldsymbol{u}(x,y)$, $\mathbf{E}(\boldsymbol{u}) = (1-\nu)\mathbf{e}(\boldsymbol{u}) + \nu\,\mathrm{div}(\boldsymbol{u})\boldsymbol{I}$, where $\mathbf{e}(\boldsymbol{u}) = (\nabla\boldsymbol{u} + {}^t\nabla\boldsymbol{u})/2$ is the "in-plane strain tensor and $\boldsymbol{I}$ is the 2D unit tensor)
- μ is the elastic shear modulus of the soft central layer.

With these variables, the comprehensive description of the out-of-plane behavior the elastic laminated plate loaded by normal surface force f is given by the following set of balance equations:

$$\mathrm{div}(\mathbf{T}) + f = 0; \qquad \mathbf{T} = -\mathrm{div}(\mathbf{M}) + \mathbf{T} \;;\qquad \mathbf{T} = -\mathrm{div}(\mathbf{M}) \qquad (2)$$

where **T** is the overall transverse shear force that balances the external load f. This set of equation expresses a bi-torsors - namely (**T**, **M**) and (**T**, **M**) - plate representation that involves the overall, and inner, shear forces and bending moments. The overall shear force **T** results from both the inner shear force **T** due to sliding and the shear force due to the proper bending of each glass layer, − div(**M**). Furthermore, **T** balances the shear force − div(**M**) due to the global bending of the whole plate.

As a consequence of the additional variable $\boldsymbol{d}$, new boundary conditions needs to be formulated. The latter conditions can be obtained by expressing the energy balance of the plate. In this view, consider a plate of surface S and of border ∂S the normal of which being **n**. The total energy developed by the deflection w under the normal loading f is given by $\int_S f.w\,\mathrm{ds}$. Transforming this expression using the balance equations (2) and twice integrations by parts, one the obtains:

$$\int_S f.w\,\mathrm{ds} = \int_S K|\nabla w - \boldsymbol{\alpha}|^2\mathrm{ds} + \int_S 2E_0 I[(1-\nu)|\mathbf{e}(\nabla w)|^2 + \nu|\mathrm{div}(\nabla w)|^2]\mathrm{ds} + \int_S 2E_0(\Im - 2I)[(1-\nu)|\mathbf{e}(\boldsymbol{\alpha})|^2 + \nu|\mathrm{div}(\boldsymbol{\alpha})|^2]\mathrm{ds}$$

$$+\int_{\partial S}(\mathbf{T}.\mathbf{n})w\,\mathrm{d}l + \int_{\partial S}(\mathbf{M}.\mathbf{n})\nabla w\,\mathrm{d}l + \int_{\partial S}(\mathbf{M}.\mathbf{n})\boldsymbol{\alpha}\,\mathrm{d}l \qquad (3)$$

On the right hand side of (3), the integrals over S express successively, the deformation energy due to the shear of the interlayer, the inner bending of each layer and the overall bending of the plate. The integrals over ∂S in (3) express the energy provided at the border. They disclose the proper boundary conditions to be used for the enriched plate model, that can be expressed with the introduced static variables **M**, **M**, **T**, and the kinematic variables w, ∇w, and $\boldsymbol{\alpha}$. For instance, the conditions at a free border are given by **T.n** = 0 and **M.n** = **M.n** = 0 while on a clamped part, the conditions will be $w = 0$ and $\nabla w = \boldsymbol{\alpha} = 0$, hence $\boldsymbol{d} = 0$.

2.2. Comparison with classical plates

The enriched plate model (1-2) encompasses the classical plate models that can be recovered as limit cases:

- Very soft ($\mu \to 0$) or very stiff ($\mu \to \infty$) central layer yield respectively to $\mathbf{T} \to 0$ or $\nabla w \to \boldsymbol{\alpha}$, that corresponds to the bi-layer Kirchhoff plate of double inertia 2I, for which $\mathbf{T} = -\mathrm{div}(\mathbf{M})$, or to the monolithic Kirchhoff plate of global inertia ℑ and shear force $\mathbf{T} = -\mathrm{div}(\mathbf{M} + \mathbf{M}) = -\mathrm{div}(E_0\Im.\mathbf{E}(\boldsymbol{\alpha}))$,
- As for inertia, when $I \to 0$, then $\mathbf{M} \to 0$ and the inner bending effect disappears. Hence, a Reissner-Mindlin model is recovered ; conversely when $\Im \to \infty$, then $\boldsymbol{\alpha} \to 0$ so that the inner bending motion dominates which results in a Shear-Bending Sandwich model.

2.3. Contrasted plate with viscoelastic interlayer

In harmonic motions ($e^{i\omega t}$) the above model directly applies to plates with viscoelastic constituents provided that the physical variables are expressed in the frequency domain e. g. $w(x, y, t) = w(x,y).e^{i\omega t}$, and that the elastic parameters are replaced by the complex-valued frequency dependent viscoelastic parameters.

As for laminated glass, the PVB interlayer only is viscoelastic of complex modulus $\mu(\omega)$, thus the single modification consists in rewriting $\mathbf{T}$ as $\mathbf{T} = \mu(\omega)(h+c)\mathbf{d}/c = K(\omega)(\nabla w - \boldsymbol{\alpha})$, the moment constitutive laws (1a) and (1c) and the balance equations (2) remaining unchanged. Note that, as presented in the Appendix, the shear modulus of the PVB varies drastically with the frequency f and the temperature θ. Typical values are of 0.1GPa for $\theta < 0°C$ and $f > 1kHz$, and of 0.1 MPa for for $\theta > 50°C$ and $f < 10^{-4}Hz$. These values, much smaller than the elastic modulus of the glass E = 74GPa, justify the modelling of the laminated glass as a contrasted plate.

In the time domain, the formulation is obtained by inverse Fourier transform. Thus, denoting $K(t) = \mu(t)\ (h+c)^2/c$ where $\mu(t)$ is the inverse Fourier transform of $\mu(\omega)$, the constitutive law of $\mathbf{T}$ involves a convolution product ($*$), and consequently, memory effects

$$\mathbf{T}(t) = K(t)*(\nabla w - \boldsymbol{\alpha}) = \int_{-\infty}^{t} K(t-\tau).(\nabla w - \boldsymbol{\alpha})(\tau)\,d\tau$$

To sum up, the out-of-plane behavior of the laminated glass is governed by a synthetic quasi-analytic formulation that corresponds to a generalized plate model with an enriched kinematics. Furthermore, the model accounts for the viscoelastic properties of the PVB interlayer. It applies to permanent, harmonic or transient loadings and can be extended easily to non-symmetric laminates cf. (Boutin and Viverge, 2016).

3. Bending waves in contrasted plates

In dynamic harmonic regime ($e^{i\omega t}$) the body force is the inertial force that reads $\rho w_{,tt} = \rho\omega^2 w e^{i\omega t}$ where ρ stands for the surface density of the laminate. Combining the constitutive laws (1) and the balance equations (2) while keeping the deflection w as the single variable yield, after simplifying by $e^{i\omega t}$, the following Tri-Laplacian equation:

$$E_0 2I.E_0(\Im - 2I).\Delta^{(3)}w - E_0\Im K.\Delta^{(2)}w + E_0(\Im - 2I)\,\rho\omega^2.\Delta w - K\,\rho\omega^2.w = 0 \qquad (4)$$

Furthermore, reporting the constitutive laws (1) in equation (2c) enables to relates ∇w and $\boldsymbol{\alpha}$ by the differential equation:

$$K\nabla w = K\boldsymbol{\alpha} - E_0(\Im - 2I)[(1-\nu)\Delta(\boldsymbol{\alpha}) + (1+\nu)\nabla\mathrm{div}(\boldsymbol{\alpha})]/2 \qquad (5)$$

Let us investigate the cylindrical bending waves propagating along the x-axis. In that case

$$w(x,y,t) = we^{kx}e^{i\omega t},$$

where k is the frequency dependent real or complex wave number. Reporting this expression in the Tri-Laplacian equation (4) and simplifying by $we^{i\omega t}$ provides the following dispersion equation:

$$E_0 2I.E_0(\Im - 2I).k^6 - E_0\Im K.\,k^4 - E_0(\Im - 2I)\,\rho\omega^2 k^2 + K\rho\omega^2 = 0 \qquad (6)$$

Introducing the following parameters that take complex and frequency dependent values if the constitutive materials are viscoelastic:

$$A = K/[E_0(\Im - 2I)]\ ;\quad B = K/(E_0 2I)\ ;\quad C = \rho\omega^2/K\ ;$$

equation (4) is rewritten as the following cubic equation for k^2:

$$(k^2)^3 - (k^2)^2(A+B) - k^2 BC + ABC = 0 \qquad (7)$$

Hence, in such laminated plates characterized by three kinematic descriptors there is there types of bending waves characterized by the roots of the dispersion equation (7). Before investigating the case of glass with viscoelastic interlayer, it is instructive to consider first the case of elastic contrasted plate.

4. Bending waves and eigen modes of elastic contrasted plates

4.1. The three types of bending waves in elastic contrasted plates

In the case of elastic constituents, the above parameters A, B and C takes real and constant values. Then, the dispersion equation (7) can be solved through the Cardan method by setting $k^2 = \gamma + (A+B)/3$. Doing so, γ is the root of the cubic equation:

$$\gamma^3 - 3P\gamma - 2Q = 0\ ;\qquad P = [(A+B)^2/3 + BC]/3\ ;\qquad Q = [(A+B)\{2(A+B)^2/9 + BC\} - ABC]/2$$

Accounting from the fact that A, B, and C are positive, analytical developments show that, whatever the frequency, the determinant $\Delta = P^3 - Q^2$ is positive. Consequently, the dispersion equation for k^2 has three real roots $\lambda_1 < \lambda_2 < \lambda_3$. Furthermore, since:

$$\lambda_1 + \lambda_2 + \lambda_3 = A+B > 0 \; ; \qquad \lambda_1\lambda_2 + \lambda_3\lambda_1 + \lambda_3\lambda_2 = -BC < 0 \; ; \qquad \lambda_1\lambda_2\lambda_3 = -ABC < 0 \tag{8}$$

the root λ_1 is negative while λ_2 and λ_3 are positive. Their expression is given by

$$\lambda_p = k_p^2 = (A+B)/3 + 2\sqrt{P}\cos[\{\arccos(Q/\sqrt{P^3}) + 2p\pi\}/3] \quad ; \; p = 1, 2, 3$$

The negative root $\lambda_1 = k_1^2$ yield a propagative wave $e^{\pm i\delta_1 x}$ of real wave number $\delta_1 = \sqrt{-k_1^2}$ and velocity $c = \omega/\delta_1$. The two other waves are evanescent $e^{\pm\delta_p x}$, characterized by the inverse attenuation length $\delta_2 = \sqrt{k_2^2}$ and $\delta_3 = \sqrt{k_3^2}$. All these waves numbers are non-linearly frequency dependent and consequently the waves are dispersive. Note also that the wave parameters of the evanescent waves are linked to the one of the propagative wave by the relation:

$$\delta_p^2 = (\delta_1^2 + A + B)[1 \mp \sqrt{1 - 4\left(1 + \frac{\delta_1^2}{A}\right)^{-1}\left(1 + \frac{A+B}{\delta_1^2}\right)^{-1}}] \tag{9}$$

The plate kinematics of each type of waves is provided by equation (5) that simplifies into $Ak_p w = (A - k_p^2)\alpha$ for cylindrical bending. Thus, for the propagative wave $e^{-i\delta_1 x}$ we have

$$\nabla w = -i\delta_1 w \; ; \qquad \alpha = \nabla w/(1 + \delta_1^2/A) \quad ; \qquad d/(h+c) = \nabla w\, \delta_1^2/(A + \delta_1^2)$$

so that, the gradient of deflection ∇w, the overall rotation α and the sliding d are in phase quadrature with the deflection, while d and ∇w are in phase. Conversely for the evanescent waves $e^{-\delta_p x}$,

$$\nabla w = -\delta_p w \; ; \qquad \alpha = \nabla w/(1 - \delta_p^2/A) \quad ; \qquad d/(h+c) = -\nabla w\, \delta_p^2/(A - \delta_p^2)$$

thus, α and d are respectively in phase and in phase opposition with the deflection w.

The occurrence of three bending waves is specific to the contrasted plates. Indeed, the dispersion equations of classical plate models leads to two types of waves, one being propagative the other evanescent. This is evidenced form the dispersion equation (5) by considering the limit cases:

- For very soft central layer ($K \to 0$) equation (5) simplifies into $k^2(k^4 - BC) = 0$ that gives the physical wave numbers of the bi-layer Kirchhoff model $\delta_1 = \pm(\rho\omega^2/(E_0 2I))^{1/4}$ and $\delta_2 = \pm i\delta_1$,
- For stiff central layer ($K \to \infty$) and equation (5) reduces to $-k^4(A+B) + ABC = 0$. Then the wave numbers are those of the monolithic Kirchhoff model $\delta_1 = \pm(\rho\omega^2/(E_0\Im))^{1/4}$ and $\delta_2 = \pm i\delta_1$,
- For weak layer inertia ($I \to 0$), one obtains the quadratic dispersion equation $-A k^4 - k^2 C + AC = 0$ of the Reissner-Mindlin plate (Reissner 1995), leading to a real wavenumber $\pm\delta_1$ and a imaginary wavenumber $\pm\delta_2 \neq \pm i\delta_1$,
- For strong overall inertia ($\Im \to \infty$) one recovers the dispersion equation of the Shear-bending sandwich plate $k^2(k^4 - B k^2 - BC) = 0$ for real and a imaginary wavenumbers $\pm\delta_2 \neq \pm i\delta_1$ are derived.

4.2. Eigen modes of an elastic contrasted plate

The determination of the eigen modes of an elastic contrasted plate submitted to given boundary conditions, follows the usual approach, except that three bending modes are involved. As an example let us focus on the case of a rectangular plate of height H, width B, clamped on the base (x = 0), free on the top (x= H), and free on the lateral sides (y = ±B/2). Accordingly, the plate experiences a cylindrical bending and the kinematic variables read:

$$w = w_{1c}\mathrm{ch}(i\delta_1 x) + w_{1s}\mathrm{sh}(i\delta_1 x) + \sum_{p=2,3}[w_{pc}\mathrm{ch}(\delta_p x) + w_{ps}\mathrm{sh}(\delta_p x)]$$

$$\nabla w = [w_{1c}\mathrm{sh}(i\delta_1 x) + w_{1s}\mathrm{ch}(i\delta_1 x)]i\delta_1 + \sum_{p=2,3}[w_{pc}\mathrm{sh}(\delta_p x) + w_{ps}\mathrm{ch}(\delta_p x)]\delta_p$$

$$\alpha = [w_{1c}\mathrm{sh}(i\delta_1 x) + w_{1s}\mathrm{ch}(i\delta_1 x)]i\delta_1/(1 + \delta_1^2/A) + \sum_{p=2,3}[w_{pc}\mathrm{sh}(\delta_p x) + w_{ps}\mathrm{ch}(\delta_p x)]\delta_p/(1 - \delta_p^2/A)$$

Now, since in cylindrical bending, $M = 2E_0 I w_{,xx}$, $T = K(w_{,x} - \alpha)$, $M = E_0(\Im - 2I)\alpha_{,x}$ and $T = -M_{,x} + T$, one has:

$$M = 2E_0 I[-[w_{1c}\mathrm{ch}(i\delta_1 x) + w_{1s}\mathrm{sh}(i\delta_1 x)]\delta_1^2 + \sum_{p=2,3}[w_{pc}\mathrm{ch}(\delta_p x) + w_{ps}\mathrm{sh}(\delta_p x)]\,\delta_p^2\,]$$

$$\mathsf{M} = \mathrm{E}_0(\Im\text{-}2\mathrm{I})[-[w_{1c}\mathrm{ch}(i\delta_1 x) + w_{1s}\mathrm{sh}(i\delta_1 x)]\delta_1^2(1+\delta_1^2/A) + \sum_p [w_{pc}\mathrm{ch}(\delta_p x) + w_{ps}\mathrm{sh}(\delta_p x)]\delta_p^2(1-\delta_p^2/A)]$$

$$\mathsf{T} = -\rho\omega^2[-[w_{1c}\mathrm{sh}(i\delta_1 x) + w_{1s}\mathrm{ch}(i\delta_1 x)]i\delta_1^{-1} + \sum_{p=2,3}[w_{pc}\mathrm{sh}(\delta_p x) + w_{ps}\mathrm{ch}(\delta_p x)]\delta_p^{-1}]]$$

Then, expressing the clamping condition on x = 0, i.e., $w(0) = \nabla w(0) = \alpha(0) = 0$, and the free conditions on x = H, i.e., $\mathsf{M}(\mathrm{H}) = \mathsf{M}(\mathrm{H}) = \mathsf{T}(\mathrm{H}) = 0$ yields a homogeneous linear set S of 6 equations of unknowns the coefficients w_{pc} and w_{ps}, p = 1, 2, 3. The latter system admits non trivial solutions when its determinant is null. The condition Det(S) = 0 gives the following equation:

$$\sum_{p=1}^{3}\left(2\frac{k_p^2k_{p+1}^2}{c_pc_{p+1}} + t_pt_{p+1}k_pk_{p+1}(k_p^2+k_{p+1}^2)\right)(k_p^4-k_{p+1}^4)^{-1} + \sum_{p=1}^{3}\frac{k_p^4(k_{p+1}^4-k_{p+2}^4)}{(k_p^4-k_{p+1}^4)(k_{p+2}^4-k_{p+3}^4)} = 0 \qquad (10)$$

in which $k_1 = i\delta_1$, $k_2 = \delta_2$, $k_3 = \delta_3$, $c_p = \mathrm{ch}(k_pH)$, $t_p = \mathrm{th}(k_pH)$, and by convention $p+i$ is the integer modulo-3. Using the relations (9) the equation Det(S) = 0 can be recast into an equation where $\delta_1 H$ is the single unknown. The resolution leads to an infinite set of wave numbers $\{\delta_{1J}, \mathrm{J\ integer}\}$. Once δ_{1J} is determined the δ_{pJ} of the evanescent waves are obtained from the relation (9). Finally, using either relations (8-b) or (8-c) that relies the roots to the inertia parameter C enables to determine the corresponding eigen frequency $\{\omega_J, \mathrm{J\ integer}\}$. As usual each of them is associated with an eigen mode w_J defined from the coefficients w_{pc} and w_{ps} solution of S at $\{\delta_{pJ}\}$.

5. Bending waves and eigen modes in laminated glass plates

As for laminated glass, due to the viscoelastic behavior of the thin PVB interlayer, $\mu(\omega)$, then $K(\omega)$, take frequency dependent complex values. Consequently, the three roots of the dispersion equation (7) are also frequency dependent and complex valued. Nevertheless, the Cardan method still enables to determine the wave numbers. As the latter are complex valued, the propagative bending wave is attenuated and the evanescent waves present spatial oscillations. The variables describing the plate kinematics of the three modes are all out phase and their ratio varies according to the frequency.

On the other hand, additional difficulties arise for determining the eigen modes and frequencies. This relies on the facts that (i) the frequency dependence of $\mu(\omega)$ makes that the parameters of the equations are themselves dependent on the researched eigen frequency, (ii) the complex value of $\mu(\omega)$ yield complex eigen modes and frequencies, (iii) the lack of analytical expression of $\mu(\omega)$ avoid to develop an analytical resolution. For these reasons the dynamics properties can only be determined numerically or using an approximated approach as presented hereafter.

The idea is that, meanwhile the PVB can have a significant loss factor, the global loss of the mechanical system constituted by the thin PVB layer embedded in the thick stiff elastic glass layers is certainly much lower. Thus the viscoelastic effect should appear as a perturbation of the elastic configuration and can be assessed by iterated approximations. The procedure detailed hereafter will be applied and compared to experiments in the section 6.

5.1. Iterated determination of the fundamental mode

The fundamental frequency ω_0 of the laminated glass plate necessarily lies in between the fundamental frequencies of the bi-layer plate model ω_b, that would correspond to $\mu = 0$, and of the monolithic plate model ω_m that that would correspond to $\mu = \infty$. For clamped/free boundary conditions, ω_b and ω_m take well known expressions. Since the PVB layer is very thin (c << h) then $\Im = 8\mathrm{I}$ and $\omega_m = 2\omega_b$ with $\omega_b = [1.2\pi/(2\mathrm{H})]^2(2\mathrm{E}_0\mathrm{I}/\rho)^{1/2}$.

Thus, $\omega_b < \omega_0 < 2\omega_b$, and $\mu(\omega)$ lies in between $\mu(\omega_b)$ and $\mu(2\omega_b)$. According to the PVB properties recalled in the appendix, such a range of frequency is sufficiently narrow to have limited variations of $\mu(\omega)$. To go further, a first frequency assessment ω_{01} is made by calculating the eigen frequency of a plate with an elastic interlayer of shear modulus $|\mu(\omega_0)|$. Then, this procedure is reiterated with $|\mu(\omega_{01})|$ to obtain a second assessment ω_{02}, etc. It appears that the convergence to the approximate value ω_{0a} is very fast, three iterations giving a relative deviation of the frequency less than 10^{-3}.

Finally, to check the relevancy of the approximation, a viscoelastic calculation is performed with the complex shear modulus $\mu(\omega_{0a})$. The three complex wave numbers are first determined and compared to the elastic ones to verify that they are only slightly modified. Then they are reported into the eigen frequency equation (10) and one verifies that the rest is negligible compared to both summed terms $\sum_{p=1}^{3}(-)$ appearing in (10)

5.2. Assessment of the damping of the fundamental mode

The damping of vibrations is an important issue, in particular for the acoustic performance of laminated glass plates. It results from the dissipation of energy by viscous effects in the PVB and therefore the elastic plate models, by nature,

fails to report it. To assess the damping of the fundamental mode one starts with the energy balance (3) at the fundamental frequency ω_0. Considering clamped/free boundary conditions the balance reads:

$$\int_S \rho\omega_0^2 w_0^2 ds = \int_S K(\omega_0)(w_{0,x} - \alpha_0)^2 ds + \int_S 2E_0 I(w_{0,xx})^2 ds + \int_S E_0(\Im - 2I)(\alpha_{0,x})^2 ds \quad (11)$$

in which $K(\omega_0) = Kr(\omega_0) + iKi(\omega_0)$ and w_0 and α_0 stand for the deflection and the overall rotation of the fundamental mode. The terms $Kr(\omega_0)(w_{0,x} - \alpha_0)^2$ and $Ki(\omega_0)(w_{0,x} - \alpha_0)^2$ correspond respectively to the elastic and dissipative part of shear deformation of the PVB.

The damping factor ζ of the mode is classical defined as 2ζ = (Dissipated energy)/(Stored elastic energy), and consequently:

$$2\zeta = [\int_S Ki(\omega_0)(w_{0,x} - \alpha_0)^2 ds]/[\int_S Kr(\omega_0)(w_{0,x} - \alpha_0)^2 ds + \int_S 2E_0 I(w_{0,xx})^2 ds + \int_S E_0(\Im - 2I)(\alpha_{0,x})^2 ds] \quad (12)$$

Note that the damping vanishes in the following cases:

- $Ki(\omega_0) = 0$, that corresponds to an elastic interlayer,
- $K(\omega_0) \to 0$, that corresponds to an elastic bi-layer plate ($\mu = 0$) ,
- $(w_{0,x} - \alpha_0) \to 0$, that corresponds to an elastic monolithic plate, ($\mu = \infty$).

Thus, one may expect that the damping presents a maximum for an "intermediate" value of $\mu(\omega_0)$ not very weak so that the amount of viscous dissipation is not negligible, but also not very large so that the sliding *d* and then the shear deformation of the PVB is not avoided.

An assessment of ζ is provided by using the eigen mode obtained at the elastic approximation ω_{0a} of the eigen frequency, instead of the proper eigen mode.

6. Experiments

The vibration experiments realized on glass plates follows two objectives. First, identify qualitatively the phenomena, and specially the role of the PVB on the dynamics with a focus on the frequency and temperature influences. Second compare the experimental data with the theoretical predictions given by the enriched plate model.

6.1. Experimental set-up

The experiments have been conducted on a plate of 600mm length, 200mm width. The laminated glass is made of two layers, each of thickness h = 18.5mm, and a PVB interlayer of 1.8mm. The plate lies vertically and is clamped on the basis of a vibrating table. It is set in bending motion by the horizontal oscillations of the table that are controlled by a laser vibrometer. The plate is equipped of two miniaturized accelerometers, one located on the top, the other on the assumed node of the second mode. In addition, a temperature sensor is glued on the plate.

The dynamic tests consist in imposing a logarithmic sweep of frequency (0-800Hz) at a constant level of table acceleration a = 12m/s^2. Before realizing each test, the plate is put in a controlled thermal chamber up to reach a stabilized temperature at the fixed value. In the present experimental campaign 17 temperatures has been tested lying between 30°C and 50°C. Considering the large thermal inertia of glass, the time needed to perform the dynamic test is sufficiently short to to keep the plate at a constant temperature (as checked by the thermal surface censor). The standard signal treatment of the accelerometric records enables to extract the transfer function (relatively to the table motion), the mode frequency and the damping at different temperatures.

6.2. Experiments versus theory

Figure 1a displays the modulus of the transfer function of the two accelerometers for a test realized at 31°C. The two first eigen frequencies are clearly identified at 74.5Hz and 460Hz. As expected, the sensor located on the node of the second modes does not detect the corresponding pick. On Figure 2a, the transfer functions of the top accelerometer in the frequency range (0-120Hz) are presented for the 17 tests realized at different temperatures. The significant influence of the temperature is clearly observed:

- the fundamental frequency moves from 74.5Hz at 31°C to 54.4Hz at 49.5°C. This reduction results from the softening of the PVB with both the increase of temperature and decrease of frequency. Note that, according to the PVB properties given in Appendix on Figure 3, the shift factor between 30°C to 50°C is of 1/250, and in turn the shear modulus is reduced from about 10^8Pa to 2.10^7Pa,
- the damping ratio actually varies non monotonically with the temperature since ζ = 8.7% at 31°C, ζ = 5.3% at 49.5°C, while at 38.5°C, ζ reaches a maximum of 13.4%. These differences are straightforwardly visible on the magnitude of the peak amplifications. Remark also that the loss in the laminated glass is much lower that that of the PVB (at 50Hz at 50°C the real and imaginary part are almost equal, see Figure 3)

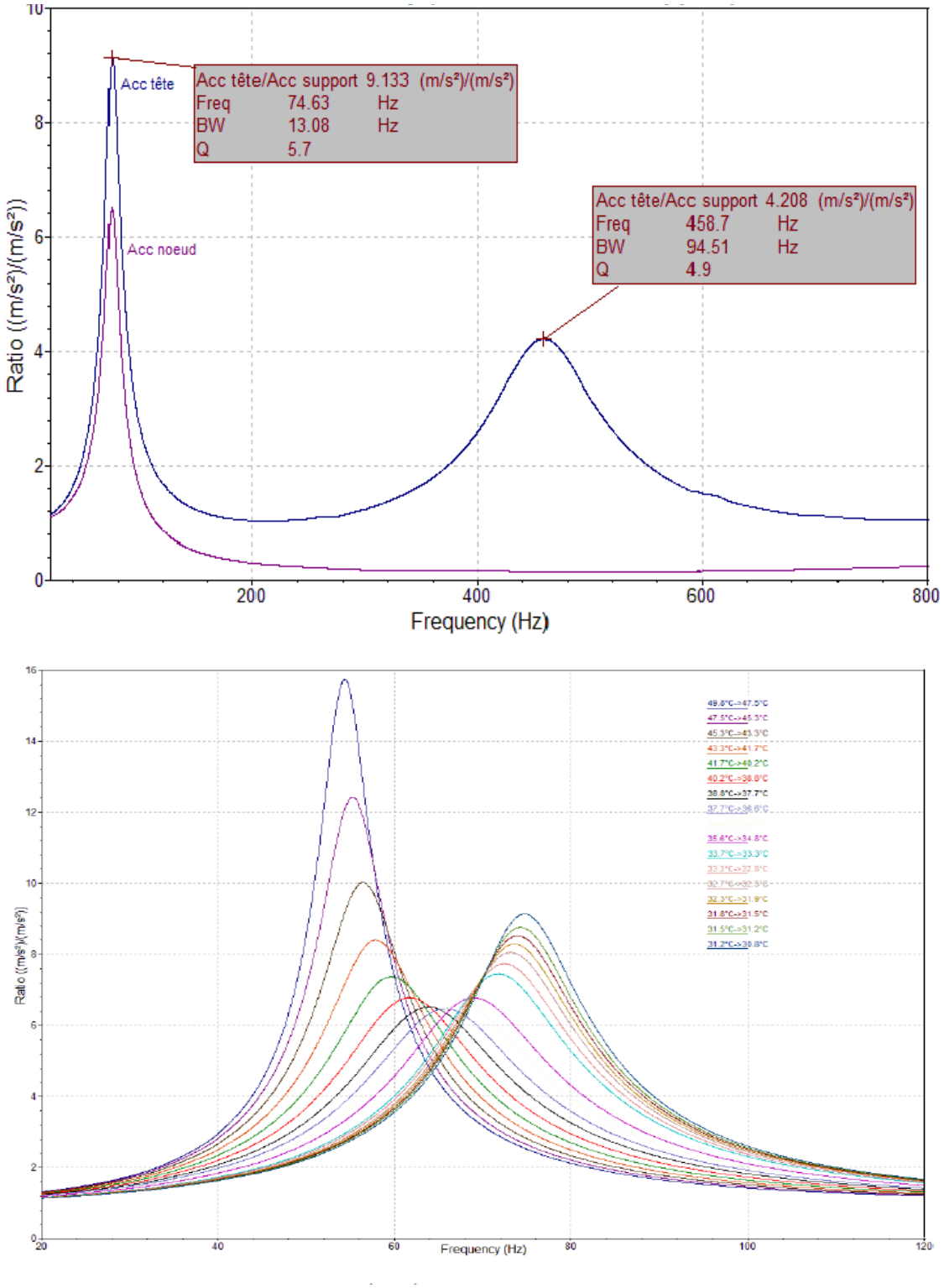

Fig. 1 Experimental transfer functions. Top : Identification of the two first eigen frequencies at a temperature of 31°C. Bottom : Identification of the fundamental frequency at different temperatures ranging from 31°C (peak at 74.5Hz) to 49.5°C (peak at 54.4Hz).

The comparison with the theoretical values is presented on Figure 2a for the fundamental frequencies, and on Figure 2b for the damping. It can be noticed a good qualitative and quantitative agreement. The damping seems quite well assessed. The experimental frequency actually lies in between the two limit frequencies corresponding to the bi-layer and monolithic Kirchhoff plate, however the experimental value is systematically lower than the theoretical one. A very likely explanation of this mismatch is that the clamping condition was not exactly reached despite the careful

realization of the device. An other possibility could be the heating of the PVB submitted to cycles, which have actually been observed trough infrared

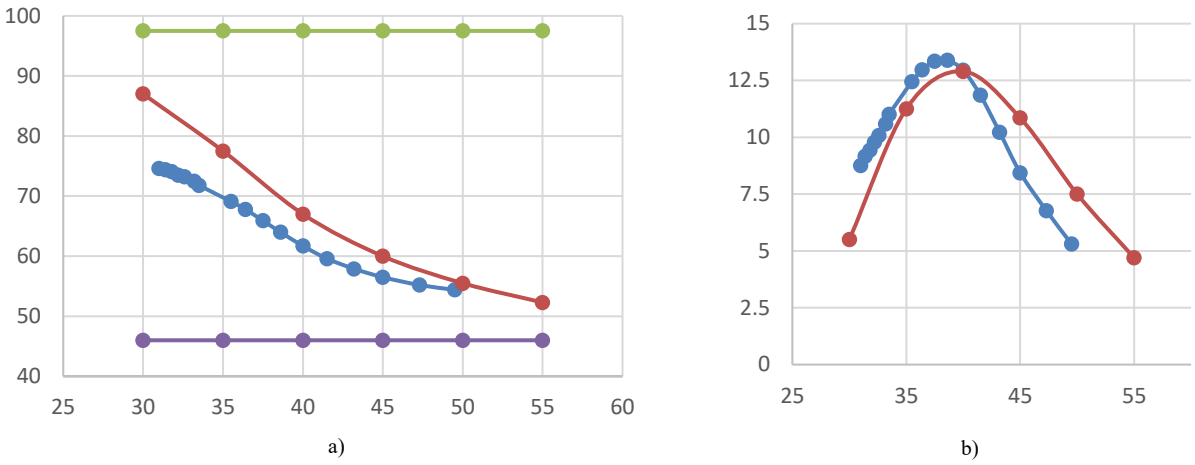

Fig. 2 Theory versus experiment for fundamental bending mode at different temperatures ranging from 30°C to 55°C. a) Fundamental frequencies; 17 blue dots: experiments; 5 red dots theory; the top and bottom lines are the fundamental frequency of respectively the monolithic and the bi-layer Kirchhoff plate. b) Damping versus temperature; 17 blue dots: experiments; 5 red dots theory.

7. Conclusion

The dynamic experiments performed on laminated glass are in good qualitative and quantitative agreement with the theoretical predictions. In particular, the influence of the temperature is well captured and is shown to be quite significant. These experimental data gained in dynamics together with those previously acquired in statics and transient regimes (Viverge et al, 2016) confirms the relevancy of contrasted plate model (1-2). A major advantage of this (quasi)-analytical model, is its physical basis that enables a clear mechanical understanding in terms of the bi-torsor formulation and the corresponding kinematic descriptors. Furthermore, compared to purely numerical approach it provides a simplest and less cost expansive way of modelling. Indeed, the numerical difficulties encountered for correctly account of the thin and soft PVB layer are overcome through the effective plate model in which they are already encapsulated.

Thus, the contrasted plate model provides a simple easy-to-use theoretical framework for engineering purposes. For instance, it allows simple comparisons of the mechanical performances - in time and temperature - of laminated glasses made with other polymeric layers than the PVB. In acoustics a straight forward application is the assessment or the improvement of the sound attenuation by laminated glass.

8. References

Auriault, J.L., Boutin, C. Geindreau, C.: Homogenization of Coupled Phenomena in Heterogeneous Media, ISTE and Wiley (2009)
Berdichevsky, V.L.: An asymptotic theory of sandwich plates. Int. J. Eng. Sci. 48, pp. 383-404 (2010)
Boutin, C., Viverge, K.: Generalized plate model for highly contrasted laminates. Eur. J. Mech. A. Solids, 55, pp. 149-166 (2016)
Viverge, K., Boutin, C., Sallet, F.: Model of highly contrasted plates versus experiments on laminated glass. Int. J. Solids Struct. 102-103, pp 238-258 (2016)
Caillerie, D.: Thin elastic plates of periodic structure with comparable period and thickness. C.R. Acad. Sci. Paris, 294II pp. 159-162 (1982)
Carrera, E.: Historical review of zig-zag theories for multilayered plates and shells. Appl. Mech. Rev. 56, 3,pp. 287-308 (2003)
Carrera, E., Ciuffreda, A.: Bending of composites and sandwich plates subjected to localized lateral loading: A comparison of various theories Compos. Struct. 68 pp.185-202 (2005)
Ciarlet, P.G., Destuynder, P.: A justification of the two-dimensional linear plate model. Journal de Mécanique, 18 pp. 315-344 (1979)
Ciarlet, P.G .: Theory of plates - Mathematical elasticity Vol.2, North-Holland (1997)
Foraboschi, P.: Analytical model for laminated-glass plate. Composites: Part B 43 pp. 2094-2106 (2012)
Galuppi, L., Royer-Carfagni, G.: Laminated beams with viscoelastic interlayer. Int. J. Solids Struct. 49,18, pp. 2637-2645 (2012)
d'Haene, P., Savineau, G.: Mechanical properties of laminated safety glass. FEM study. Glass peformance day - Finland (2007)
Ivanov, I.V.: Analysis, modelling, and optimization of laminated glasses as plane beam. Int. J. Solids Struct. 43, pp. 6887-6907 (2006)
Sanchez-Palencia, E.: Non Homogeneous Media and Vibration Theory, Springer-Verlag, Berlin (1980)
Reissner, E.: Reflexion on the theory of elastic plates. Appl. Mech. Rev. 38, pp.1453-1464 (1995)

Appendix : PVB properties

The PVB interlayer is a polymer that presents viscoelastic properties. In harmonic regime $e^{i\omega t}$ at temperature θ, the shear modulus μ(ω, θ) is complex valued, i.e. μ = The real and imaginary parts μ_r and μ_I correspond respectively to the elastic and to the loss moduli. Like most of polymers, PVB follows the principle of time-temperature superposition.

Hence, $\mu(\omega, \theta)$ depends on the reduced variable $\omega\tau_\theta$, where τ_θ, is a temperature dependent characteristic time. The latter is related to the characteristic time at the reference temperature θ_0 by the relation $\tau_\theta = \tau_{\theta_0} a_\theta$, where a_θ is a time dependent function characteristic of the PVB. Thus, the knowledge of (i) the frequency dependence of $\mu(\omega, \theta_0)$ at the reference temperature θ_0 and of (ii) the shift factor a_θ, allows determining the viscoelastic properties at any frequency and temperature since $\mu(\omega, \theta) = \mu(\omega a_\theta, \theta_0)$. These two properties are depicted on Figure 2 (from experiments of d'Haene and Savineau 2007).

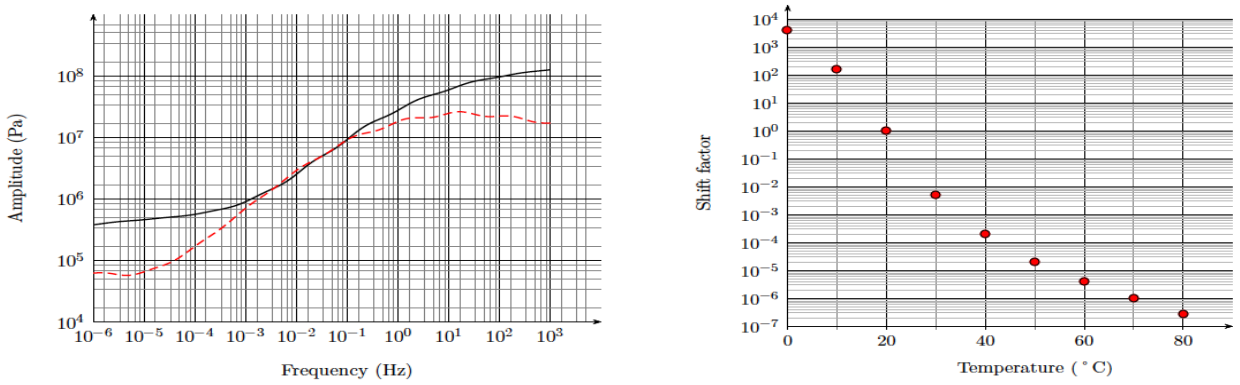

Fig. 3 Viscoelastic properties the PVB. Left : Shear modulus μ versus frequency ; Elastic μ_r (line) and loss μ_i (dashed) modulus at the temperature $\theta = 30°C$. Right : Shift factor $a\theta$ versus temperature.

Challenging Glass 7
Conference on Architectural and Structural Applications of Glass
Belis, Bos & Louter (Eds.), Ghent University, September 2020.
ISBN 978-94-6366-296-3, www.challengingglass.com

PLATINUM SPONSORS

GOLD SPONSORS

SILVER SPONSORS

ORGANISING PARTNERS